Vol. 686: 159–175, 2022
https://doi.org/10.3354/meps13985

MARINE ECOLOGY PROGRESS SERIES
Mar Ecol Prog Ser

Published March 24

Oxygen isotope fractionation in otoliths: experimental results from four North Pacific and Arctic gadid species

Craig R. Kastelle[1,*], Thomas E. Helser[1], Benjamin J. Laurel[2], Louise A. Copeman[2,3], Kali R. Stone[1], Jennifer L. McKay[4]

[1]Resource Ecology and Fisheries Management Division, Alaska Fisheries Science Center, National Marine Fisheries Service, NOAA, Seattle, WA 98115, USA

[2]Fisheries Behavioral Ecology Program, Hatfield Marine Science Center, Alaska Fisheries Science Center, National Marine Fisheries Service, NOAA, Newport, OR 97365, USA

[3]Hatfield Marine Science Center, College of Earth, Ocean, and Atmospheric Sciences, Oregon State University, Newport, OR 97365, USA

[4]College of Earth, Ocean, and Atmospheric Sciences, Oregon State University, Corvallis, OR 97331, USA

ABSTRACT: High-latitude climate warming is expected to have wide-ranging effects on habitats, ecosystems, and the fish species that occupy them. Not all fish species will be able to adapt to increasing temperatures. We investigated oxygen isotope fractionation in fish otoliths and its relationship to environmental temperature and thermal histories of individual fish. Fish from 4 gadid species, *Gadus macrocephalus*, *Boreogadus saida*, *Eleginus gracilis*, and *G. chalcogrammus*, representing North Pacific and Arctic regions, were reared in a range of controlled temperatures (0–20°C). We estimated 4 new species-specific otolith oxygen isotope fractionation equations, a relationship between otolith $\delta^{18}O$ and temperature (T) in the form $\delta^{18}O_o - \delta^{18}O_w = m \times T°C + b$ and also in a second form using the fractionation factor α: $1000 \ln \alpha = a \times (1000\ TK^{-1}) + c$, where o is otolith, w is water, and m, b, a and c are regression coefficients. In using the first form, *B. saida* was the most unique among the 4 species, with the steepest slope (–0.23) and the highest intercept (32.99‰ Vienna PeeDee Belemnite [VPDB]). *G. macrocephalus* had the lowest slope (–0.17) and the lowest intercept (31.76‰ [VPDB]). Results of an ANCOVA test indicated that the 4 fractionation equations were not statistically different ($F = 2.25$, $p > 0.087$). However, when we applied the 4 new fractionation equations to $\delta^{18}O_o$ measured in wild-caught *B. saida* otoliths, the species-specific fractionation equation resulted in the closest match between measured and predicted water temperatures. These new fractionation equations represent new tools for investigating temperature effects on fish biota and will also improve paleotemperature reconstruction, especially for high-latitude species.

KEY WORDS: Oxygen isotope fractionation equation · Temperature · Otolith · Climate change · Thermal exposure history · Arctic cod · Pacific cod · Saffron cod · Walleye pollock

1. INTRODUCTION

Thermal experience influences every life history aspect of fishes and is a fundamental variable in ecosystem studies and fisheries management. The impacts of global climate change on fish communities are forecasted to be most severe in Arctic and boreal ecosystems (Hoegh-Guldberg & Bruno 2010, Hollowed et al. 2013, Burrows et al. 2014, Vestfals et al. 2016), but the rates and degree of impact largely depend on what thermal habitats fish use and how these variable thermal conditions influence meta-

*Corresponding author: craig.kastelle@noaa.gov

bolic processes such as fish growth, condition, and recruitment (Koenker et al. 2018, Laurel et al. 2018). Controlled experimental studies have shown that a species' marginal or unavailable thermal preference can affect fish growth and health (Laurel et al. 2016b, Copeman et al. 2017). Some species are expected to adapt (regional movements or prey species shifts) or move poleward as climate warming occurs, while others do not have that adaptive ability due to specific habitat or prey requirements (Hollowed et al. 2013, Fossheim et al. 2015). For example, the Pacific cod population in the Gulf of Alaska suffered a 71% decline in abundance which was likely due to an extreme warming event in 2014 to 2016 (Barbeaux et al. 2020). Knowing and understanding thermal histories of wild fish is especially challenging in mobile fish species, such as gadid species, with access to multiple thermal environments over space, time, and development stage. In Arctic and boreal regions, gadids are key links in the ecosystem, such as in food chains, and can also be an indicator species in the face of environmental shifts due to climate change. Further, sampling fish in winter habitats, with substantial ice cover as in the Arctic, may not be feasible. Hence, to better understand the wide-ranging effects of increasing high-latitude temperatures, new and accurate tools for reconstructing thermal histories in key species are necessary.

Otoliths are often used to provide broad environmental information, and a wider diversity of otolith analyses are being incorporated into ecological–population–climate studies. The otoliths of teleost fish are calcium carbonate structures, in the form of aragonite, which are part of the fish's inner ear. They are an acellular metabolically inert structure that is formed as calcium carbonate and is continuously deposited onto a proteinaceous matrix (Campana 1999, Wright et al. 2002, Hussy et al. 2004, Popper et al. 2005). In teleost fish, otoliths grow continuously throughout the life of the fish in such a way that pairs of translucent and opaque layers are deposited each year (Campana & Thorrold 2001, Thomas & Swearer 2019). Calcium carbonate makes up about 95% of the otolith, and the remaining portion is protein (Degens et al. 1969, Thomas et al. 2019). The otolith's properties, in the form of other trace chemical, isotopic, or radionuclide content, can often be used as proxies for a wide range of ecological information (e.g. Miller et al. 2005, Tracey et al. 2017, Benson et al. 2019, Matta et al. 2019, Andrews et al. 2020, Kastelle et al. 2020). Stable isotopes in otoliths, our focus here, can provide ecological information, such as fish thermal exposure history, fish age, migrations, metabolism, and feeding (e.g. Thorrold et al. 1997, Schwarcz et al. 1998, Weidman & Millner 2000, Hoie et al. 2003, Hoie & Folkvord 2006, West et al. 2012, Darnaude et al. 2014). Hence, otoliths can be used as recording devices which contain a wide range of life history information for individual fish (Elsdon et al. 2008).

In fish otoliths, and other marine biogenic calcareous material, the fractionation of stable oxygen isotopes is largely a function of temperature. The ratio of ^{18}O:^{16}O in the otolith (expressed in the international standard delta notation of $\delta^{18}O$ [Brand et al. 2014, Darnaude et al. 2014]) is inversely related to the ambient temperature (summarized by Thorrold et al. 1997, Campana 1999, Darnaude et al. 2014). However, the otolith's $\delta^{18}O$ is also a function of $\delta^{18}O$ in the ambient water, which in turn is related to salinity (Spero & Lea 1996, Dorval et al. 2011, Wright 2013, Darnaude et al. 2014). The relationship between temperature and fractionation can be expressed as a linear relationship (referred to as a fractionation equation) as follows:

$$1000 \ln \alpha = a \times (1000\ T\mathrm{K}^{-1}) + c \quad (1)$$

where T is temperature in K, and a and c are regression coefficients. The isotopic fractionation factor α is:

$$\alpha = \frac{\delta^{18}O_o + 1000}{\delta^{18}O_w + 1000} \quad (2)$$

where o and w refer to $\delta^{18}O$ in the otolith and water, respectively. This relationship (Eq. 1) can be expressed in the form of a second-order polynomial, as was done by Godiksen et al. (2010) and Hoie et al. (2004). This relationship can also be expressed in a second form as:

$$\delta^{18}O_o - \delta^{18}O_w = m \times T°\mathrm{C} + b \quad (3)$$

where T is temperature in °C, and m and b are regression coefficients. In Eqs. (2) & (3), the $\delta^{18}O_w$ of the ambient water can be measured, estimated by a proxy such as salinity, or determined by a variety of methods (e.g. modeled from an environmental database [Darnaude et al. 2014] or presumed from measurements made at a different time or from a nearby location [Gao et al. 2001, Hoie & Folkvord 2006, Hanson et al. 2013]).

When a specific functional relationship between $\delta^{18}O_o$ in otoliths and temperature is known (i.e. Eqs. 1 or 3), and the $\delta^{18}O_w$ is known or estimated, the $\delta^{18}O_o$ can be used as a proxy for the water temperature in which a fish lived. For this reason, the oxygen isotopic composition of otoliths has been used as a tool in a wide range of ecological and environmental ap-

plications. For example, $\delta^{18}O_o$ measured in otoliths recovered from archeological sites was used to estimate coastal seawater paleotemperatures (Geffen et al. 2011, West et al. 2012, Helser et al. 2018a). More commonly, otoliths from recently captured fish have been used to estimate the temperatures experienced by a fish (e.g. Jones & Campana 2009, Dorval et al. 2011, Horn et al. 2012, Darnaude et al. 2014, Hane et al. 2020, von Leesen et al. 2020). Ecologically, Higuchi et al. (2019) related oxygen isotopes in larval and juvenile chub mackerel *Scomber japonicas* to somatic growth, age, and annual recruitment. Jones & Campana (2009) used stable oxygen isotopes to determine that Atlantic cod *Gadus morhua* made small-scale thermoregulatory migrations and experienced temperature-related growth changes. The $\delta^{18}O_o$ was used in discriminating between substocks of plaice *Pleuronectes platessa* (Darnaude et al. 2014, Darnaude & Hunter 2018). Understanding the thermal histories of wild-caught fish, by using otoliths and an established fractionation equation, offers a powerful tool to identify habitat and temperature preferences that support fitness and survival at early life stages or to support other considerations such as paleotemperature research. This is important because a number of laboratory studies have shown species-specific relationships between temperature variation and subadult growth, survival, and metabolic processes of Arctic and boreal gadid species (Laurel et al. 2016a,b, 2018, Copeman et al. 2017, Koenker et al. 2018). These growth and survival processes in relation to temperature highlight the reason for our type of study.

The fractionation of oxygen isotopes in otoliths can also be used to study the life history of individual fish. If an otolith can be sampled across its growth zones (i.e. from hatching to capture) at a high spatial resolution, then cyclical $\delta^{18}O_o$ chronologies, which are assumed to be highly correlated to seasonal cyclical temperature fluctuations, can be used as a robust proxy for true age. These life history chronologies have been used in Pacific cod *G. macrocephalus* (Kastelle et al. 2017), pike *Esox lucius* (Gerdeaux & Dufour 2012), and Atlantic cod (Weidman & Millner 2000).

The wide range of examples of temperature reconstruction and ecological investigations demonstrate the usefulness of this relationship between $\delta^{18}O_o$ and temperature, but central considerations in these applications remain. Importantly, it is widely suggested that the functional relationship (i.e. fractionation equation) is species specific and may vary geographically (e.g. Thorrold et al. 1997, Hoie et al. 2004, Storm-Suke et al. 2007, Godiksen et al. 2010, Geffen 2012, Darnaude et al. 2014, Sakamoto et al. 2017, Willmes et al. 2019). Well-established fractionation equations relating $\delta^{18}O_o$ and water temperature (Eqs. 1 & 3), developed specifically for the species and region being studied, are necessary in applications of otolith thermography to account for such variations. The central premise is that $\delta^{18}O_o$ is in equilibrium with seawater (Thorrold et al. 1997), but divergence from this equilibrium could exist (i.e. the otolith aragonite does not precipitate in oxygen isotopic equilibrium with its environment) (Thorrold et al. 1997, Hoie et al. 2004, Storm-Suke et al. 2007, Godiksen et al. 2010, Geffen 2012, Darnaude et al. 2014, Sakamoto et al. 2017, Willmes et al. 2019). If so, then species-specific temperature-dependent fractionation equations should be developed. To that end, fractionation equations are often developed by using temperatures estimated from related environmental data or *in situ* temperature measurements, both of which can be difficult to obtain (e.g. Storm-Suke et al. 2007, Hanson et al. 2013, Darnaude et al. 2014, Helser et al. 2018a). Developing a fractionation equation also requires data from a wide temperature range. A reliable solution is laboratory controlled-temperature studies (e.g. Thorrold et al. 1997, Hoie et al. 2004, Hoie & Folkvord 2006, Geffen 2012).

In the North Pacific and Arctic oceans, 4 gadid species are ecologically important: Pacific cod *G. macrocephalus*, Arctic cod *Boreogadus saida*, saffron cod *Eleginus gracilis*, and walleye pollock *Theragra chalcogramma*. Pacific cod and walleye pollock support large commercial fisheries in Alaska waters; in 2018, they represented US$ 701.5 million in ex-vessel value (Fissel et al. 2019). These gadids have shown changes in growth, condition, and recruitment in response to temperature variation (Laurel et al. 2016b, Copeman et al. 2017, Koenker et al. 2018, Barbeaux et al. 2020). Hence, we chose these 4 species for this current research because they are likely to be affected by climate change and can also be considered an important example of broad environmental indicators; however, determining the way in which they are affected requires an understanding of growth related to environmental temperatures.

In this study, our focus was oxygen isotope fractionation in the calcium carbonate (aragonite) of otoliths and its relationship to environmental temperature in controlled thermal environments. Our first goal was to develop new fractionation equations for the 4 gadid species from the North Pacific and Arctic oceans. This component relied on a laboratory experiment where fish were reared at a range of controlled temperatures.

In this first component, we also expand on a fractionation equation previously developed from field collections (Kastelle et al. 2017). Our second goal was to test and compare the effects of the 4 new fractionation equations on predicted temperatures. In this second component, we used $\delta^{18}O_o$ measured in wild-caught Arctic cod otoliths. By measuring $\delta^{18}O_o$, and using newly established species-specific fractionation equations, the temperature history of wild-caught fish can be related to important ecological and fisheries management questions related to somatic growth (Jones & Campana 2009, Higuchi et al. 2019), temperature preference, or stock discrimination (Jones & Campana 2009, Darnaude et al. 2014).

2. MATERIALS AND METHODS

2.1. Sample source and laboratory experiment

The otoliths used here were from juvenile fish in a controlled-temperature rearing study measuring temperature-dependent growth (Laurel et al. 2016b) and lipid accumulation (Copeman et al. 2017) at the Hatfield Marine Science Center in Newport, OR, USA. The fish were originally captured in the spring and summer of 2013 before being transported to the Hatfield Marine Science Center laboratory. The capture locations for Arctic cod and saffron cod were in the Beaufort Sea (in Prudhoe Bay, AK, USA), those for Pacific cod were in the Gulf of Alaska (near Kodiak, AK, USA), and those for walleye pollock were in the Puget Sound (Port Townsend, WA, USA) (Fig. 1). After an acclimation period of 2 to 3 mo at 6 to 8°C, juvenile fish were placed into rectangular tanks (66 × 46 × 38 cm, 3 individuals per species per tank) and acclimated to temperature treatments of 0, 5, 9, 16, and 20°C over a period of 2 d (2 tanks per temperature treatment). After the acclimation period, the rearing study lasted 6 wk. The temperature range of 0 to 16°C reflects the potential variation in summer temperatures experienced by these boreal and Arctic gadids, which can reside in cold offshore Arctic regions or warmer shallow boreal areas (Copeman et al. 2017); a warm treatment, 20°C, at which some of the species could survive was also included (Laurel et al. 2016b). During the 6 wk study, temperature and salinity (controlled-temperature flow-through seawater) were recorded every 15 min; the average temperatures were –0.18 ± 0.32, 5.24 ± 0.17, 8.93 ± 0.19, 16.19 ± 0.21, and 19.83 ± 0.19°C (mean ± SD). The salinity averaged 32.85 ± 0.55 for Arctic cod and saffron cod and averaged 33.13 ± 0.63 for Pacific cod and walleye pollock. The seawater, and hence salinity, did not vary between temperature treatments within any 1 species. Additional juvenile Arctic cod and saffron cod were acclimated to a 2°C temperature treatment using the same protocol and experimental design. All fish during the experimental phase were fed the same iso-caloric gel food diet to satiation. The temperature–lipid study lasted 6 wk, after which the fish were sacrificed and the otoliths removed and stored in a 70% ethanol solution. To determine the growth rates for individual fish, each fish was tracked and measured at the beginning and end of the 6 wk study (Laurel et al. 2016b). Up to 8 and, due to mortalities, as few as 3 fish from each temperature–species combination were collected (Table 1). Further details of the handling procedure and experimental design of the growth study are provided in Laurel et al. (2016b) and Copeman et al. (2017).

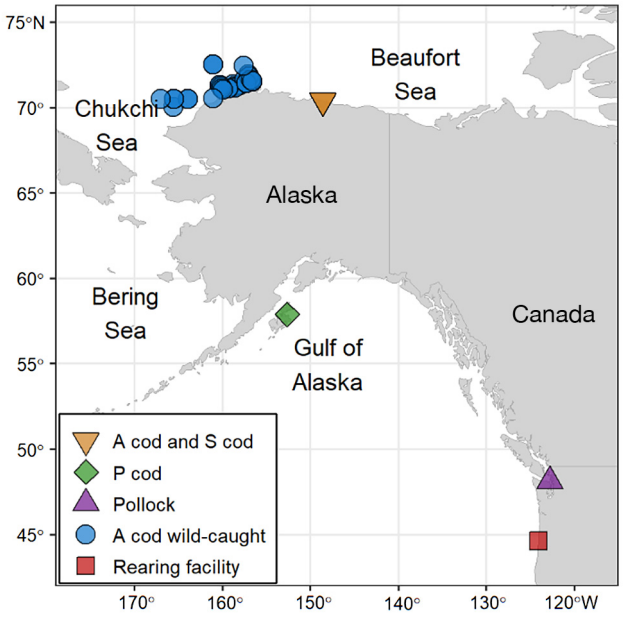

Fig. 1. Capture areas for experimental fish and wild-caught test fish. The experimental samples are Arctic cod and saffron cod (A cod and S cod, respectively), Pacific cod (P cod), and walleye pollock. The test fish are wild-caught Arctic cod (A cod wild-caught). The rearing facility at Newport, OR, USA, is also shown. Note that the experimental samples of Arctic cod and saffron cod are from the same location

2.2. Otolith analysis and mass spectrometry

After storage in ethanol for up to a year, the otoliths were cleaned in a sonic cleaner with milli-Q water, dried at 70°C for 24 h, and weighed. The whole otoliths were then bonded, proximal side up, to glass mi-

Table 1. Summary of specimens by species and temperature treatment: number of specimens, otolith mass, fish length at the end of the experiment, mass of otolith material milled for analysis, average daily percent growth rate and average $\delta^{18}O$ for each species and temperature treatment for each of the 4 species: Pacific cod *Gadus macrocephalus*, Arctic cod *Boreogadus saida*, saffron cod *Eleginus gracilis*, and walleye pollock *Theragra chalcogramma* subjected to temperature treatments and used for otolith $\delta^{18}O$ fractionation equations. Average fish length and growth rate are taken from Laurel et al. (2016b) and Copeman et al. (2017). na: not available

Species and temperature (°C)	No. of specimens successfully analyzed for $\delta^{18}O$	Average otolith mass (mg)	Average milled sample mass (µg)	Average fish length (mm)	Average growth rate (%, mass d^{-1})	Average $\delta^{18}O$ (95% CI) (‰, VPDB)
Arctic cod *Boreogadus saida*						
0	8[a]	7.374	46	100	0.65	2.24 (0.02)
2	8	6.622	44	95	0.59	2.02 (0.02)
5	8	8.825	40	109	1.24	1.19 (0.02)
9	8	12.628	58	120	1.10	0.34 (0.02)
Walleye pollock *Theragra chalcogramma*						
0	6	4.208	39	65	0.29	1.33 (0.04)
5	6	7.134	40	84	1.30	0.84 (0.04)
9	6	9.063	34	96	2.17	−0.08 (0.04)
16	5	11.687	35	99	2.58	−1.49 (0.03)
20	6	14.424	48	95	na	−2.25 (0.04)
Saffron cod *Eleginus gracilis*						
0	6[a]	20.025	45	98	0.24	0.98 (0.04)
2	5	21.909	54	na	na	1.36 (0.03)
5	5	22.168	43	111	0.89	1.11 (0.03)
9	6	23.974	47	106	1.43	0.48 (0.04)
16	4	28.215	51	120	1.93	−0.85 (0.02)
20	5	28.014	46	132	1.05	−1.70 (0.03)
Pacific cod *Gadus macrocephalus*						
0	2	6.493	31	66	0.67	1.04 (0.02)
5	6	12.989	39	97	1.72	0.72 (0.02)
9	6	20.159	39	117	2.59	−0.58 (0.01)
16	3	14.337	34	99	2.01	−1.35 (0.01)
20	3	18.081	36	88	na	−2.06 (0.01)

[a]One Arctic cod and 6 saffron cod were suspected to be outliers and not included; see Section 3

croscope slides with Loctite 349 UV curing glue (Henkel) (Fig. 2). The glue did not extend to the outer edge of the otolith but was only placed under the center of the distal side. A Carpenter Microsystems CM-2 micromill was used to sample the otoliths. The micromill consisted of a computer-actuated XYZ slide stage, a fixed-position 0.3 mm ball head milling bit, a stereo microscope, and a high-resolution digital camera, all of which were interfaced and guided by specialized software (Carpenter Microsystems CM-2). This is the same system used by Kastelle et al. (2017) and Helser et al. (2018b). The longer dorsal and ventral edges provided the simplest region to mill, so the stage was guided such that these edges were sampled (Fig. 2). To

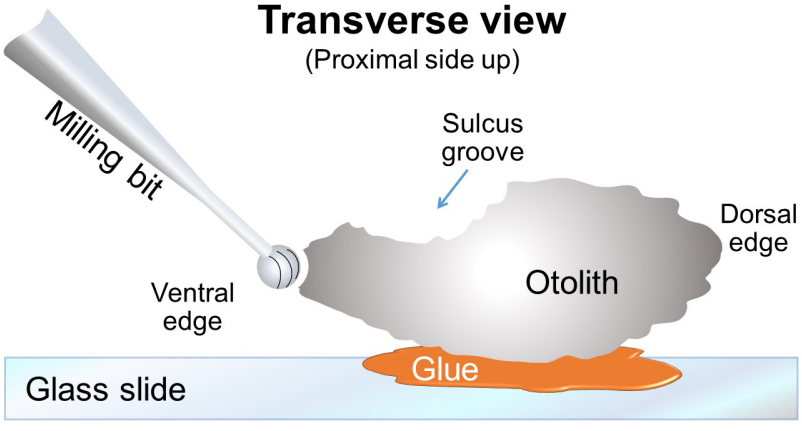

Fig. 2. Stylized transverse view of a whole otolith, from the temperature treatment study, mounted on a glass slide, and includes a milling bit; the anterior–posterior axis is perpendicular to the plane of the image. The otolith's proximal side is facing up, and dorsal and ventral edges are the right and left ends, respectively

get the quantity required for mass spectrometry (about 30 µg), milling usually extended the full length of the otolith, anterior to posterior, and less than 20 µm into the otolith's edge. This method of micromilling, which critically limited the depth milled into the otolith's edge, was designed to sample only otolith material deposited during the 6 wk of the temperature treatment study, while still providing sufficient material for analysis. Milling depth into the otolith's edge was based on the milling system's high-resolution control and calibrated measurements (Fig. S1 in the Supplement at www.int-res.com/articles/suppl/m686p159_supp.pdf). Copeman et al. (2017) reported fish length ranges by species, across all temperature treatments, before and after the experiment. All 4 species demonstrated increased length ranges; Pacific cod and walleye pollock had the largest increases. We expected otolith growth in proportion to fish growth (Helser et al. 2017); hence, the milling depth of 20 µm should represent only new material deposited during the experiment. The milled powder was collected with microspatulas while viewed under the microscope and sealed in clean stainless steel cups (4 mm wide and 4 mm deep) prior to analysis. The milling bit and microspatulas were cleaned between each sample with a 3 mm wide stiff hair brush and compressed air to avoid cross contamination.

The sample material generated by edge milling was analyzed by isotope ratio mass spectrometry (IRMS) at the Oregon State University's College of Earth, Ocean, and Atmospheric Sciences Stable Isotope Laboratory for $\delta^{18}O_o$ following the same methods as Kastelle et al. (2017) and Helser et al. (2018b). Briefly, the system utilized was a Kiel III carbonate preparation system (Thermo Scientific), where each sample was reacted with 105% orthophosphoric acid at 70°C, coupled to a MAT 252™ dual-inlet isotope ratio mass spectrometer (Thermo Scientific). The analysis of otolith samples was bracketed by multiple evaluations of the standard NBS-19 (US Geological Survey, Reston, VA, USA) and an internal lab standard (previously calibrated with NSB-18 and NSB-19). The repeat measurements of the internal lab standard were used to calculate 95% CIs. The accuracy was evaluated by repeat measurements of NBS-19. Finally, the otolith oxygen isotopic measurements were adjusted using an acid fractionation factor of 1.0090898, which was calculated by Kim et al. (2007). No correction for sample size (i.e. mass correction) was made because the standards and samples were of similar size; however, occasionally a drift correction was applied if warranted based on a comparison of standards at the beginning and end of the run. The results are reported in standard delta notation, $\delta^{18}O_o$ relative to Vienna Pee Dee Belemnite (VPDB).

2.3. Calculations and statistical analysis

Ambient $\delta^{18}O_w$ was estimated from salinity for use in calculating fractionation equations (Eqs. 1 & 3). Spero & Lea (1996) developed the following relationship for the California Bight between $\delta^{18}O_w$ relative to Vienna Standard Mean Ocean Water (VSMOW) and salinity:

$$\delta^{18}O_w\,(\text{VSMOW}) = 0.39 \times \text{Salinity} - 13.46 \quad (4)$$

Estimating $\delta^{18}O_w$ from salinity is broadly geographically specific (Fairbanks 1982, Weidman & Millner 2000, Harwood et al. 2008, Jones & Campana 2009, Yamamoto-Kawai et al. 2010, Darnaude et al. 2014, Conroy et al. 2017, Higuchi et al. 2019). The published relationship of Eq. (4) (Spero & Lea 1996) is appropriate for our study because both the California Bight and Hatfield Marine Science Center are in the California Current Large Marine Ecosystem (https://editors.eol.org/eoearth/wiki/California_Current_large_marine_ecosystem, last accessed 28 Jan 2021).

The isotopic analysis of otoliths yields $\delta^{18}O_o$ data that are on the VPDB scale. In contrast, the analysis or calculation of $\delta^{18}O_w$ (as in Eq. 4 above) yields data that are on the VSMOW scale. It is therefore necessary to convert the $\delta^{18}O_w$ values to the VPDB scale when using the fractionation equations (Eqs. 1 & 3). As per the recommendations of the Commission on Isotopic Abundances and Atomic Weights (https://www.ciaaw.org/oxygen-references.htm, last accessed 28 Jan 2021), the following equation from Brand et al. (2014) should be used:

$$\delta^{18}O_w\,(\text{VPDB}) = 0.97001 \times \delta^{18}O_w\,(\text{VSMOW}) - 29.99 \quad (5)$$

This equation is an updated version of the Friedman & O'Neil (1977) equation:

$$\delta^{18}O_w\,(\text{VPDB}) = 0.97006 \times \delta^{18}O_w\,(\text{VSMOW}) - 29.94 \quad (6)$$

It is important to note that, for decades, many otolith studies (e.g. Kalish 1991, Hoie et al. 2004) have incorrectly used a $\delta^{18}O_w$ (VSMOW) to VPDB correction factor of −0.22 (e.g. $\delta^{18}O_w$ [VPDB] = 0.99978 × $\delta^{18}O_w$ [VSMOW] − 0.22), which was incorrectly attributed to Friedman & O'Neil (1977). This correction factor is simply the difference between the $\delta^{18}O_w$ (VSMOW) of the CO_2 gas when equilibrated with standard mean ocean water and the $\delta^{18}O_w$ (VSMOW) of CO_2 released from the carbonate reference material Pee

Dee Belemnite when it is reacted with acid (see Chapter 6 in Sharp [2007]). Hence, −0.22 should not be used as a correction factor to convert the $\delta^{18}O_w$ to the VPDB scale.

The fractionation equations were evaluated using ANCOVA in SAS 9.2. First, we fit linear regression models, using Microsoft Excel 2016, to each species individually, Eqs. (1) & (3), to estimate the relationship between the $\delta^{18}O_o$ and temperature. To test if the species-specific fractionation equations were statistically different, $\delta^{18}O_o - \delta^{18}O_w$ was regressed on temperature, species (as a class variable), and their interaction. A final model was analyzed, using the same statistical approach, to evaluate if fish growth rate (% mass d^{-1}) exhibited an effect on $\delta^{18}O_o - \delta^{18}O_w$, either individually or similarly, for the different species. Using the correct species-specific fractionation equation is an important consideration of our study. Therefore, we also compared the fractionation equations generated here to a selection of published equations from other species and areas in controlled-temperature juvenile or larval rearing experiments (Table 2). In these comparisons, an ANCOVA was not possible, but the fractionation equations were subjectively compared using reported regression coefficients. Our selection of these other studies was limited because of the history of using an incorrect $\delta^{18}O_w$ VSMOW to VPDB conversion.

Previously, Kastelle et al. (2017) reported a fractionation equation for Pacific cod from the North Pacific. In their study, they did not measure salinity or $\delta^{18}O_w$ but assumed a $\delta^{18}O_w$ of 0‰ (VSMOW) by not including it in their fractionation equation. This is not necessarily a bad assumption, but it could introduce errors into temperature predictions. In addition, the assumed 0‰ (VSMOW) should have been converted to the VPDB scale using Eq. (5). Therefore, to facilitate comparisons here, we applied this conversion to the previously determined fractionation equation and obtained the following:

$$\delta^{18}O_o\,(\text{VPDB}) - \delta^{18}O_w\,(\text{VPDB}) = -0.21 \times T°\text{C} + 33.22 \quad (7)$$

2.4. Test with wild-caught Arctic cod

To further investigate the differences between the 4 new fractionation equations, we made temperature predictions from each equation using a single data set of $\delta^{18}O_o$ from wild-caught Arctic cod. These predictions were then compared to water temperatures measured at capture. Arctic cod otoliths were collected during August and September of 2013 in an Arctic Ecosystem Integrated Survey (Arctic Eis) (Mueter et al. 2017, Vestfals et al. 2019) in the Chukchi Sea (by a combination of surface trawls and midwater trawls) and in a Shelf Habitat and EcoLogy of Fish and Zooplankton project (Logerwell et al. 2018, Copeman et al. 2020) in the Chukchi Sea (by a combination of midwater trawls and bottom trawls) (Fig. 1). From these collections, 35 specimens were chosen based on growth zone clarity and age (0–4 yr). These specimens had concurrent CTD measurements taken at 1 m depth intervals (J. Gann, S. Danielson, L. Logerwell unpubl. data). From this collection of wild-caught Arctic cod otoliths, we used 2 age groups, young-of-the-year (YOY) and 1 yr old specimens (total n = 17), for $\delta^{18}O_o$ measurements and temperature predictions (Table S1). The YOY otoliths were pulverized between 2 clean glass microscope slides, and the resulting powder was analyzed for $\delta^{18}O_o$. The 1 yr old wild-caught Arctic cod otoliths were embedded in polyester resin and mounted whole on microscope slides. The otolith's distal side was facing up at the resin surface. The whole otolith was then polished flat, parallel to the slide, making a sagittal cross section through the core (Fig. 3). The 1 yr old otoliths were then micromilled such that the resulting powder for analysis represented the summer of capture. This was done by first milling away (removing) the material which was interior to the current summer's growth. Then, the milling bit was guided through the opaque zone (representing the current summer's growth) just inside of the otolith's edge. In this procedure, the milling was not restricted to just the otolith's edge, as it was for the otoliths in the temperature treatments (Fig. 3). This micromilling followed the general procedures used by Kastelle et al. (2017) and Helser et al. (2018b), and the mass spectrometry to measure $\delta^{18}O_o$ followed the same procedures as described above for the specimens in the temperature treatments.

To make temperature predictions, we also needed to have $\delta^{18}O_w$ information or, alternatively, salinity measurements to calculate $\delta^{18}O_w$. Therefore, to best represent the salinity conditions experienced by these Arctic cod, we averaged the top 5 and bottom 5 salinity CTD measurements over all casts represented by a fish, n = 35 in all age groups, to get 1 overall average measured salinity value, which was 30.62. The salinity conditions experienced by these fish during their summer of capture are unknown; therefore, this averaging was the most parsimonious procedure. Next, we used a set of eastern Bering Sea (EBS) $\delta^{18}O_w$ measurements matched with salinity CTD measurements, n = 791 (S. Danielson unpubl. data), taken in 2008 to develop an appropriate new

Table 2. Fractionation equations given in the forms of $\delta^{18}O_o - \delta^{18}O_w$ (Eq. 3), 1000 ln α (Eq. 1), and the second-order polynomial form of Eq. (1). The first 4 sets of equations are from the species in this study, and for comparison other selected species with published equations are presented. All species and studies listed are from controlled laboratory rearing environments using fish in early life stages. In all of the equations, the $\delta^{18}O$ for both water and otolith aragonite is in the VPDB scale, based on Eq. (5). Estimated coefficients and ± SE

Source	Species, stage	Fractionation equations
This study	Arctic cod *Boreogadus saida*, juvenile	$\delta^{18}O_o - \delta^{18}O_w = -0.23\ (\pm 0.01) \times T°C + 32.99\ (\pm 0.05)$, $R^2 = 0.95$ $1000 \ln \alpha = 17.49\ (\pm 0.72) \times (1000\ TK^{-1}) - 30.54\ (\pm 2.58)$, $R^2 = 0.95$ $1000 \ln \alpha = -13.02\ (\pm 21.47) \times (1000\ TK^{-1})^2 + 111.26\ (\pm 154.59) \times (1000\ TK^{-1}) - 199.35\ (\pm 278.30)$, $R^2 = 0.95$
This study	Pacific cod *Gadus macrocephalus*, juvenile	$\delta^{18}O_o - \delta^{18}O_w = -0.17\ (\pm 0.02) \times T°C + 31.76\ (\pm 0.23)$, $R^2 = 0.79$ $1000 \ln \alpha = 13.57\ (\pm 1.63) \times (1000\ TK^{-1}) - 17.41\ (\pm 5.77)$, $R^2 = 0.79$ $1000 \ln \alpha = 2.12\ (\pm 22.34) \times (1000\ TK^{-1})^2 - 1.34\ (\pm 157.54) \times (1000\ TK^{-1}) + 8.88\ (\pm 277.65)$, $R^2 = 0.79$
This study	Saffron cod *Eleginus gracilis*, juvenile	$\delta^{18}O_o - \delta^{18}O_w = -0.17\ (\pm 0.01) \times T°C + 32.52\ (\pm 0.13)$, $R^2 = 0.92$ $1000 \ln \alpha = 14.06\ (\pm 0.90) \times (1000\ TK^{-1}) - 18.44\ (\pm 3.17)$, $R^2 = 0.91$ $1000 \ln \alpha = -30.00\ (\pm 13.97) \times (1000\ TK^{-1})^2 + 225.31\ (\pm 98.38) \times (1000\ TK^{-1}) - 390.11\ (\pm 173.10)$, $R^2 = 0.93$
This study	Walleye pollock *Theragra chalcogramma*, juvenile	$\delta^{18}O_o - \delta^{18}O_w = -0.19\ (\pm 0.01) \times T°C + 32.05\ (\pm 0.12)$, $R^2 = 0.93$ $1000 \ln \alpha = 14.93\ (\pm 0.81) \times (1000\ TK^{-1}) - 22.09\ (\pm 2.87)$, $R^2 = 0.93$ $1000 \ln \alpha = -21.32\ (\pm 10.48) \times (1000\ TK^{-1})^2 + 165.60\ (\pm 76.63) \times (1000\ TK^{-1}) - 288.11\ (\pm 135.32)$, $R^2 = 0.94$
Willmes et al. (2019)	Delta smelt *Hypomesus transpacificus*, juvenile	$\delta^{18}O_o - \delta^{18}O_w = -0.19\ (\pm 0.01) \times T°C + 31.34\ (\pm 0.09)$, $R^2 = 0.96$ $1000 \ln \alpha = 18.39\ (\pm 0.43) \times (1000\ TK^{-1}) - 34.56\ (\pm 1.49)$, $R^2 = 0.94$
Hoie et al. (2004)[a]	Atlantic cod *Gadus morhua*, juvenile	$1000 \ln \alpha = 16.75\ (\pm 01.33) \times (1000\ TK^{-1}) - 27.09\ (\pm 4.62)$, $R^2 = 0.94$ $1000 \ln \alpha = 28.15\ (\pm 21.99) \times (1000\ TK^{-1})^2 - 180.00\ (\pm 153.72) \times (1000\ TK^{-1}) + 316.62\ (\pm 268.55)$, $R^2 = 0.95$
Geffen (2012)	Plaice *Pleuronectes platessa*, juvenile	$1000 \ln \alpha = 15.99 \times (1000\ TK^{-1}) - 24.25$
Shirai et al. (2018)	Glass eel *Anguilla japonica*, larvae	$1000 \ln \alpha = 13.39 \times (1000\ TK^{-1}) - 16.91$, $R^2 = 0.94$
Godiksen et al. (2010)[a]	Arctic charr *Salvelinus alpinus*, juvenile	$1000 \ln \alpha = 20.43\ (\pm 01.25) \times (1000\ TK^{-1}) - 41.14\ (\pm 4.44)$, $R^2 = 0.95$ $1000 \ln \alpha = 89.90\ (\pm 27.55) \times (1000\ TK^{-1})^2 - 617.19\ (\pm 195.40) \times (1000\ TK^{-1}) + 1089.24\ (\pm 346.42)$, $R^2 = 0.97$

[a]Hoie et al. (2004) and Godiksen et al. (2010) estimated the second-order polynomial equations presented here; however, as Hoie et al. (2004) chose to do, we relied on the linear equations to provide an increased number of comparisons to previous research

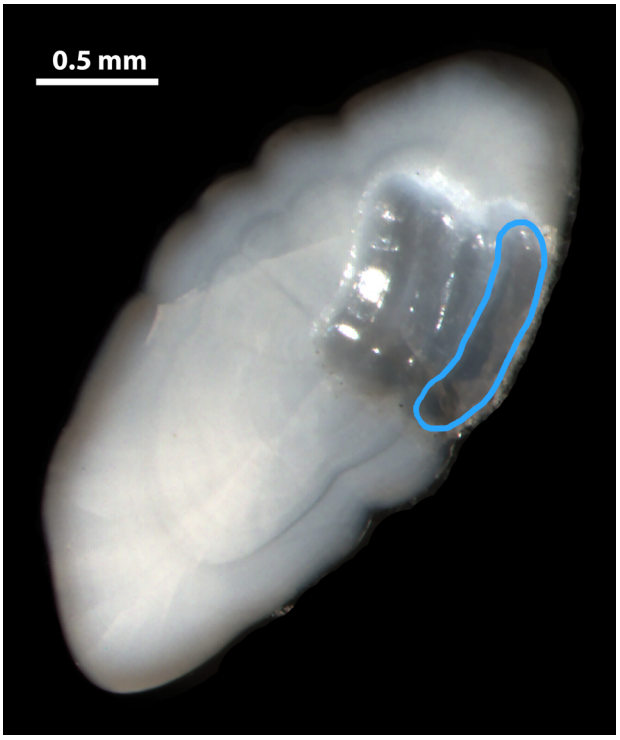

Fig. 3. Example of a 1 yr old wild-caught Arctic cod whole otolith mounted in resin, with the otolith's distal surface at the resin surface. It was polished flat to make a plane through the core (sagittal cross section). Milled material thought to be deposited during their second summer, indicated by the area outlined in blue, was sampled for $\delta^{18}O_o$ measurement. This sample included more material than just the edge

salinity mixing line to estimate an overall $\delta^{18}O_w$, which was determined to be:

$$\delta^{18}O_w \text{ (VSMOW)} = 0.474 \times \text{Salinity} - 16.324 \quad (8)$$

Finally, to calculate predicted temperatures for each YOY and 1 yr old Arctic cod, we applied the new Arctic cod fractionation equation (Table 2) to each individual Arctic cod $\delta^{18}O_o$ measurement and also used the single overall average $\delta^{18}O_w$. For comparison, we also applied the other 3 new fractionation equations from Pacific cod, saffron cod, and walleye pollock (Table 2) to each individual Arctic cod $\delta^{18}O_o$ measurement. In this way, we made 4 sets of predicted temperatures, each based on 1 of the 4 new fractionation equations.

Each set of predicted temperatures was compared to a set of common measured CTD temperatures. Each fish in the 2 age groups (YOY and 1 yr old specimens) had an associated CTD cast, so we used the average of the CTD surface and bottom temperature measurements (5 top measurements and 5 bottom measurements) to arrive at a within-fish average measured temperature. In this way, we arrived at a single common set of n = 17 within-fish average measured temperatures. This was a similar procedure to that used for the average salinity, except that in this case, it was only averaged within each fish, not over all fish. The appropriateness of each fractionation equation was considered using a paired-sample *t*-test between the predicted temperatures and the within-fish average measured temperatures.

3. RESULTS

The micromilling and IRMS was largely successful. The samples were typically above the 30 µg needed for IRMS analysis (Table 1). From all 4 species, 122 samples were analyzed with IRMS, of which 10 had insufficient mass due to material loss caused by static electricity during sample handling (Table 1). The 95% CIs of $\delta^{18}O_o$ measurements were normally less than 0.1‰ (VPDB), and the average of the standard NBS-19 (known value is −2.20‰ [VPDB]) measurements was −2.20‰ (VPDB) (n = 30 ± 0.05), indicating low variability within normal IRMS performance.

A number of specimens were considered outliers and were not used to estimate the fractionation equations. These outliers were isolated to the lowest temperature treatments where we suspected there was very little material deposited on the otoliths due to slow growth. In Arctic cod, the 1 outlier specimen from the 0°C treatment had a low $\delta^{18}O_o$ value and also had the smallest body mass, length, and otolith mass compared to other Arctic cod at 0°C. In saffron cod, all 6 specimens at 0°C were considered outliers. These specimens can be identified in Fig. 4. They were lower in body mass and length when compared to the average at other temperature treatments, and 4 of the specimens had an otolith mass less than the average at other temperature treatments. Also, the growth rate, % mass d^{-1}, of all saffron cod at 0°C was lower than other saffron cod at higher temperatures (Table 1). Because of the 2 to 3 mo acclimation period at 6 to 8°C, we suspect that the outermost layer of the otolith, represented by the 6 wk study, was thinner in the cold-temperature outliers; that is, the slower-growing fish reasonably had proportionately less deposition on their otoliths. Hence, the depth of milling likely removed material that was deposited at warmer temperatures during the acclimation period. For these reasons, these outliers were removed and not included in the fractionation equation regressions.

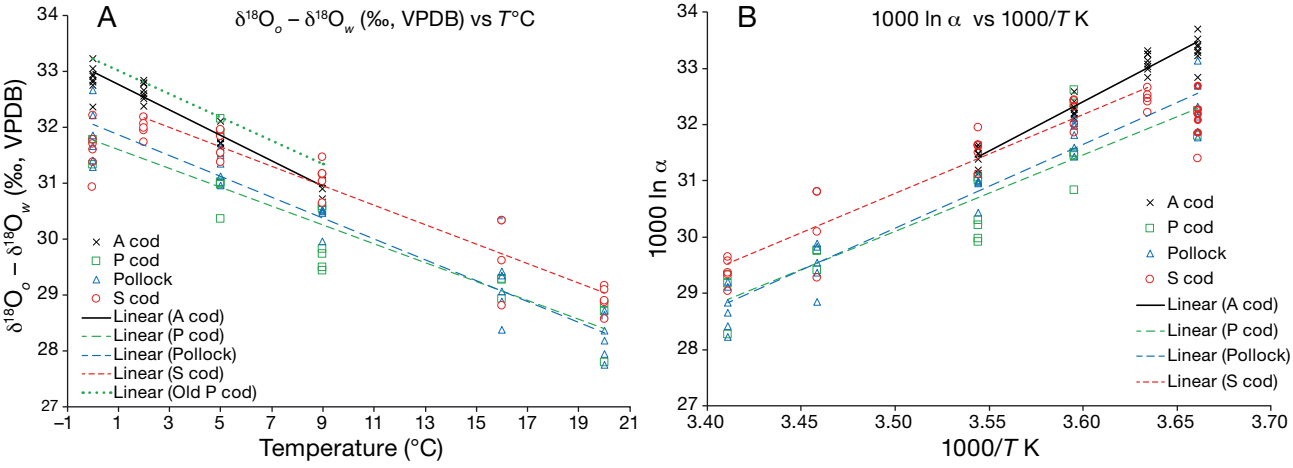

Fig. 4. Plotted $\delta^{18}O$ results and fractionation equations for each species: Pacific cod *Gadus macrocephalus* (P cod), Arctic cod *Boreogadus saida* (A cod), saffron cod *Eleginus gracilis* (S cod), and walleye pollock *Theragra chalcogramma*. Two forms of fractionation equations are shown: (A) is based on $\delta^{18}O_o - \delta^{18}O_w$ (Eq. 3), where temperature is in °C, and VPDB refers to the Vienna Pee Dee Belemnite scale. Old P cod is from Kastelle et al. (2017) and was only published in the $\delta^{18}O_o - \delta^{18}O_w$ form; (B) is based on 1000 ln α (Eq. 1), where α is the fraction factor between water and the otolith's calcium carbonate (Eq. 2), and temperature is in K (Eq. 1)

Four species-specific fractionation and temperature relationships were developed and were highly significant (using Eq. 3, Arctic cod $p = 5.9 \times 10^{-21}$, saffron cod $p = 5.4 \times 10^{-14}$, Pacific cod $p = 1.4 \times 10^{-7}$, walleye pollock $p = 4.3 \times 10^{-17}$). The 2 forms of the fractionation equations for each species are given in Table 2 and Fig. 4. Pacific cod had the lowest coefficient of determination, $R^2 = 0.79$, whereas for the other 3 species, $R^2 = 0.93$ or higher (Table 2). To develop the new fractionation equations, the average salinities and Eqs. (4) & (5) were used to estimate the $\delta^{18}O_w$, which was −30.620 ± 0.408‰ (VPDB) (±95% CI) for Arctic cod and saffron cod and −30.513 ± 0.468‰ (VPDB) (±95% CI) for Pacific cod and walleye pollock. In the 1000 ln α form, Arctic cod had the most unique fractionation equation among the 4 species, with the steepest slope (17.49) and the lowest intercept (−30.54), while Pacific cod had the lowest slope (13.57) and the highest intercept (−17.41). ANCOVA results indicated no statistical difference in the fractionation equations ($F = 2.25$, $p > 0.087$). Also, the growth rate did not have an effect on the $\delta^{18}O_o$: in walleye pollock, Arctic cod, and saffron cod, $p > 0.5$; in Pacific cod, $p > 0.07$. We also investigated second-order polynomials, based on our Eq. (1), similar to Godiksen et al. (2010) and Hoie et al. (2004) (Table 2). The second-order polynomials did not improve the coefficient of determination, R^2, estimates in the 4 gadid species (Table 2). In Arctic cod, Pacific cod, and walleye pollock, the second-order terms were not significant: $p = 0.55$, $p = 0.93$, and $p = 0.06$, respectively. In saffron cod, the second-order term was significant: $p = 0.04$. Exclusive use of second-order polynomials would have reduced the number of comparisons we made to other studies (Table 2). Hence, we only used the linear fractionation equations in these comparisons.

Our paired-sample *t*-tests using the wild-caught Arctic cod $\delta^{18}O_o$ and the 4 fractionation equations indicated that the predicted temperatures were most accurate when the correct species-specific equation was used. The average measured temperature (average of the CTD top 5 and bottom 5 measurements) for the 2 age groups was 1.60°C (Table S1). The average predicted temperature when using the Arctic cod fractionation equation was 2.16°C (Table S1), which was not significantly different from the average measured temperature ($t = 1.05$, $p > 0.2$). When using the fractionation equations for Pacific cod, saffron cod, and walleye pollock and the $\delta^{18}O_o$ from the wild-caught Arctic cod, the average predicted temperatures were all significantly different from the average measured temperatures and were −4.39°C ($t = -8.28$, $p < 3.6 \times 10^{-7}$), 0.09°C ($t = -2.16$, $p < 0.046$), and −2.44°C ($t = -6.22$, $p < 1.30 \times 10^{-5}$), respectively (Table S1). The differences between the predicted temperatures from the wild-caught Arctic cod $\delta^{18}O_o$ while using each fractionation equation and average measured temperatures are also shown in Fig. 5.

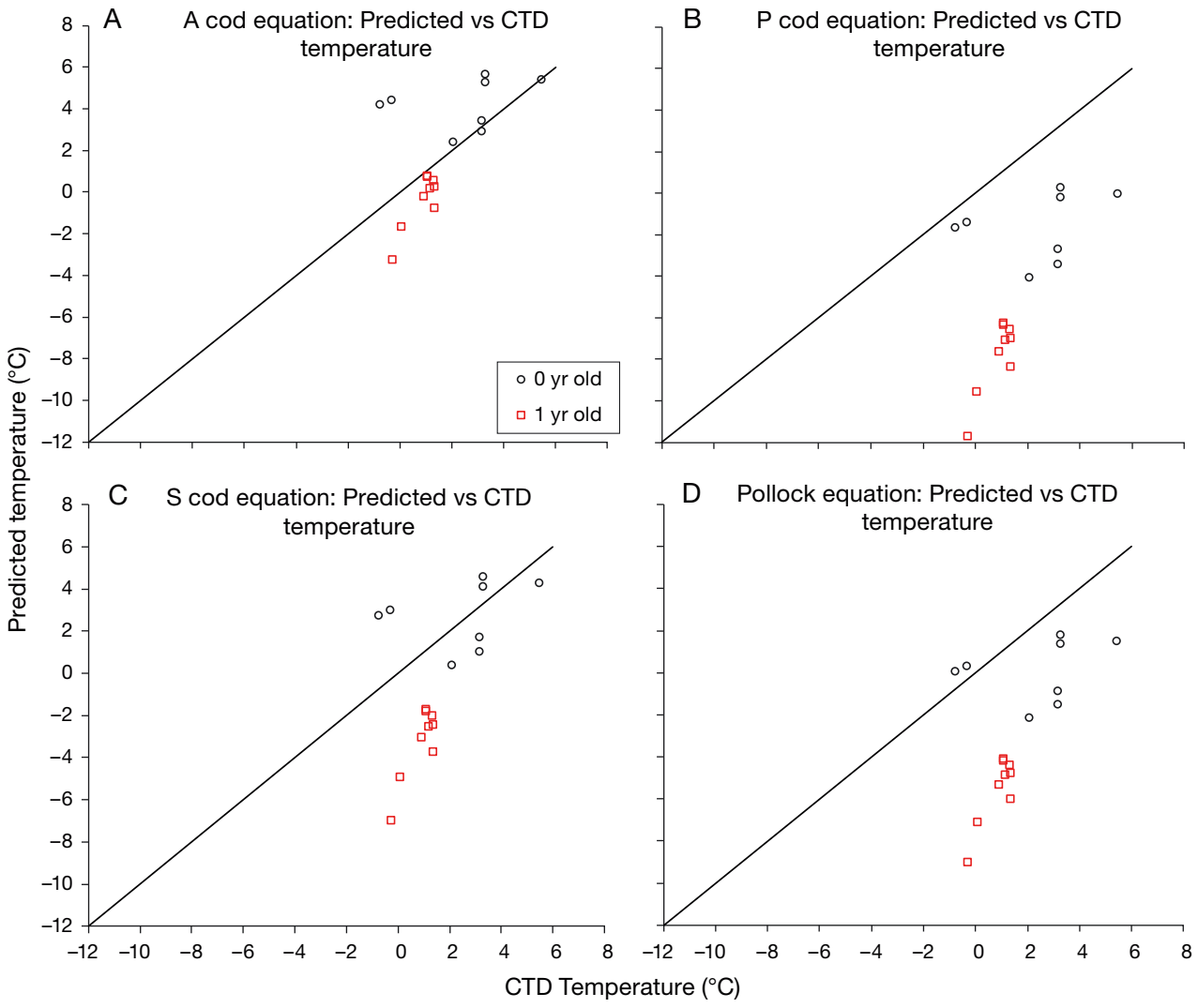

Fig. 5. Temperature (°C) predictions with the fractionation equations using $\delta^{18}O_o$ in wild-caught Arctic cod which were aged 0 yr old (young of the year) or 1 yr old, total n = 17. Using the fractionation equations in Table 2, (A) Arctic cod (A cod) $\delta^{18}O_o$ with the correct species-specific Arctic cod fractionation equation, then using the fractionation equations that were determined for (B) Pacific cod (P cod), (C) saffron cod (S cod), and (D) walleye pollock

4. DISCUSSION

Using controlled-temperature treatments in a laboratory setting, we developed 4 species-specific fractionation equations for 4 gadid species from the North Pacific and Arctic oceans. The treatments provided accurate measurements of water salinity, from which $\delta^{18}O_w$ was estimated, and controlled temperatures (Laurel et al. 2016b, Copeman et al. 2017). Both $\delta^{18}O_w$ and temperature data are necessary when developing new fractionation equations (e.g. Thorrold et al. 1997, Godiksen et al. 2010, Sakamoto et al. 2017). But direct measurements of $\delta^{18}O_w$ and temperature are sometimes not available. In that case, other sources such as regional environmental data, global environmental databases, or less accurate methods are used to arrive at temperature, $\delta^{18}O_w$, or salinity estimates (Hanson et al. 2013, Darnaude et al. 2014). For example, some data points used to estimate a fractionation equation by Kastelle et al. (2017) relied on temperature measured only at the time of fish capture, by a net-mounted instrument, and were assumed to represent the precipitation temperature of aragonite sampled from a shallow depth on the edge of the otolith. Also in this example, they did not measure salinity or $\delta^{18}O_w$ and therefore by default assumed that the $\delta^{18}O_w$ was 0‰ (VSMOW). Darnaude et al. (2014) estimated both salinity and $\delta^{18}O_w$

for individual fish from models relying on regional environmental conditions. With the controlled-temperature treatments utilized in this study, we were able to get real-time values of salinity and temperature measured accurately, which is an advantage in developing fractionation equations.

A particular strength of this study was that the 4 gadid species, representing different regions in the North Pacific and Arctic oceans, were evaluated under common environments to determine the relationships between water–aragonite oxygen fractionation in their otoliths and temperature. Controlled-temperature experiments for each species were done concurrently at the same location, with water and food from the same source (Laurel et al. 2016b, Copeman et al. 2017), during which fish growth rates were determined and salinity measurements were made to estimate $\delta^{18}O_w$. Hence, outside environmental influences on vital effects (physiological or metabolic influences) were largely removed, including source water (geographic), food (quantity and quality), and temporal or oceanographic differences that might add confounding variance in the determination of otolith oxygen isotope fractionation equations. Our study relied on juvenile fish; this also removed the potential confounding factor of different life stages. It is conceivable that these gadids have different fractionation equations as adults. Normal salinities experienced by these gadid species would likely be different and have much more variability than the salinities in this study, but the accurate salinity measurements allowed for the development of new fractionation equations. However, the $\delta^{18}O_w$, or salinity, must be known, or accurately estimated, for the application of these new fractionation equations. This unique research situation allowed us to consider predominantly inherent species-specific differences.

Based on the ANCOVA, the fractionation equations were not statistically different among the 4 species. Indeed, in Fig. 4 and Table 2, it is apparent that 3 of the species, Pacific cod, saffron cod, and pollock, have somewhat similar equations, and Arctic cod subjectively appears to have a distinctive fractionation equation; their slope and intercept were the greatest among the 4 species. While not statistically significant, this result may be biologically meaningful given their stenothermic growth pattern and unique physiological adaptions to the Arctic region, especially when compared to the boreal species, walleye pollock and Pacific cod (Drost et al. 2016, Laurel et al. 2016b).

The life history strategies of these 4 gadids have notable differences. Of the 2 Arctic species, saffron cod are eurythermic and more tolerant to higher temperatures, while Arctic cod are stenothermic and less tolerant to high temperatures (Laurel et al. 2016b). Vestfals et al. (2019) determined that in the Chukchi Sea and western Beaufort Sea, larvae and juvenile Arctic cod abundance peaked at 6°C and decreased at warmer temperatures, while larvae and juvenile saffron cod abundance increased with temperatures beyond 6°C. Typically, Arctic cod are known to spawn during the winter while they are associated with sea ice, and the eggs are buoyant and near the ice–water interface. Arctic cod larvae remain near the surface until they settle to the bottom in late summer. However, this description is a generalization, as Arctic cod use all habitats for all life history stages (summarized by Logerwell et al. 2015). The adults are found offshore in benthic shelf habitats, throughout the water column, at the ice edge, and along shorelines (Logerwell et al. 2015). Arctic cod are also known to make extensive migrations between northern summer feeding areas and southern winter spawning areas (Vestfals et al. 2019). Similarly, all life history stages of saffron cod utilize a range of habitats, but their habitat usage in the Chukchi Sea and Beaufort Sea may be different. Beaufort Sea saffron cod spawn on the shelf, and the older larvae and juveniles move into nearshore areas. In the Chukchi Sea, older saffron cod tend to be offshore, which is similar to Arctic cod (Logerwell et al. 2015). Gulf of Alaska Pacific cod YOY juveniles utilize warmer nearshore areas and ontogenetically move offshore as 1 yr olds, shifting deeper as adults (Shimada & Kimura 1994, Laurel et al. 2009, Matta et al. 2019). As adults, they are also known for making extensive spawning migrations (Shimada & Kimura 1994, Laurel et al. 2009, Matta et al. 2019). Walleye pollock are unique among these gadids; they form large schools and are semi-pelagic, including the larvae and juveniles (Brodeur et al. 1995). The implication is that these inherently different life history strategies, and responses to water temperatures, are mirrored in the somewhat different fractionation equations.

Seven specimens were excluded from further analyses, as they were considered to reflect a mixture of the acclimation period and temperature treatment period. As such, we considered these specimens to be outliers. We suggest for future studies where the specimens are subjected to cold temperatures, on the extreme end of their tolerance range, that (1) the fish be reared for a longer period (>6 wk) to ensure sufficient otolith material is deposited prior to analysis or (2) sampling (micromill) be conducted at shallower depths over a longer circumference of the otolith's

edge. The inclusion of material deposited prior to the temperature treatments, during the warmer acclimation period, would bias these specimens' $\delta^{18}O_o$ measurements low, which appears to be the case (Fig. 4). Alternatively, a sampling method which has a much higher spatial, and hence temporal, resolution on the otolith is secondary ion mass spectrometry (SIMS) (Weidel et al. 2007, Helser et al. 2018b). If SIMS had been used on the otolith's edge, some of this problem could have been avoided. However, SIMS is more expensive and less available than the IRMS we used here.

As a simple evaluation, we used the $\delta^{18}O_o - \delta^{18}O_w$ form of the fractionation equations and applied a temperature of 4°C. The predicted $\delta^{18}O_o - \delta^{18}O_w$ values were 32.08‰ (VPDB), 31.82‰ (VPDB), 31.09‰ (VPDB), and 31.30‰ (VPDB) for Arctic cod, saffron cod, Pacific cod, and walleye pollock, respectively. The differences of $\delta^{18}O_o - \delta^{18}O_w$ between the Arctic and boreal species were larger than the differences between species within either category. Notably, the difference between Arctic cod and Pacific cod is 1‰, representing a temperature difference of 1.9°C, whereas the difference between Arctic cod and saffron cod is only 0.26‰. These estimates of $\delta^{18}O_o - \delta^{18}O_w$ are not statistically different given the SEs of the coefficients in the fractionation equations (Table 2). However, the relative trends indicate that these new fractionation equations may have value for improving estimates of temperature histories. This conclusion is reinforced by our finding that fish growth rate did not affect the $\delta^{18}O_o$.

In our further testing of the 4 new species-specific fractionation equations with the wild-caught Arctic cod, the paired-sample *t*-tests indicated that the Arctic cod equation was the most accurate in predicting temperatures. The temperatures predicted with the Arctic cod fractionation equation agreed best with the measured temperatures (Fig. 5). However, there was notable variability around the 1:1 line of agreement between the predicted temperature and average measured temperatures (Fig. 5). This could have several causes. First, the otolith material sampled may not be represented by the salinity or temperature measured at the time of capture. In both age groups of wild-caught Arctic cod, the sampled otolith material (crushed whole otoliths or micromilled) represented several months; in the case of the YOY, it represented the full life of several months, and in the 1 yr olds, it represented 1 to 2 mo of summer growth (Fig. 3). The SIMS method of sampling could also have been useful in this situation. Second, we averaged the top and bottom salinity and temperature measured by the CTD instrument. We did this to account for a potential broad range of conditions experienced by the Arctic cod. But this may not represent the unknown location of the fish in the water column. It is likely that the 2 age groups had been experiencing different environmental conditions because they were in different ontogenetic stages. This may explain the differential bias of the YOY and 1 yr olds compared to the measured temperatures (Fig. 5). Both of these scenarios could be exacerbated by extreme environmental conditions in the Arctic. For example, when sea ice forms, brine is produced, and when sea ice melts, low-salinity seawater is released. This influence on $\delta^{18}O_w$ presents an additional challenge when reconstructing temperature exposures of Arctic fish. The prediction of temperature from $\delta^{18}O_o$ is sensitive to the salinity-based estimates of $\delta^{18}O_w$; a salinity change of 1 causes a 2°C change in estimated temperature. In the case of these wild-caught Arctic cod, the salinity measured by CTD ranged from about 28 to 33, and the average we used was 30.62. This value agrees with salinity ranges that were associated with higher abundance of Arctic cod late-stage juveniles in the Arctic Eis survey (Vestfals et al. 2019). Given the results of the test with wild-caught Arctic cod and the considerations above, we propose that the Arctic cod species-specific fractionation equation is the most parsimonious choice of the 4 possibilities. Further, we suggest that this confirms the importance of using species-specific fractionation equations when predicting environmental temperatures from $\delta^{18}O_o$.

Our development of a new salinity mixing line for the EBS, Eq. (8), provides a geographically appropriate conversion. The conversion of salinity to $\delta^{18}O_w$ using Eq. (4), which represented the California Bight (Spero & Lea 1996), was likely not appropriate for the EBS and further north. Given the sensitivity of temperature predictions to $\delta^{18}O_w$, this is a valuable tool. Future research using otoliths from the EBS and Chukchi Sea to make temperature predictions will benefit from this new relationship.

A comparison of our species-specific fractionation equations, which were developed under controlled laboratory conditions, to field-based fractionation equations demonstrated apparent differences. We adjusted the fractionation equation previously developed for Pacific cod by Kastelle et al. (2017) to account for $\delta^{18}O_w$ and arrived at Eq. (7), which is included in Fig. 4A for comparison. The slope of this previous equation is greater than that estimated here for Pacific cod but within the range of the other 3 gadids. However, the previous intercept in Eq. (7) is

higher than that estimated here for Pacific cod and also higher than the other 3 gadids. Their fractionation equation was estimated with a mix of adult fish from the Gulf of Alaska extending into the Aleutian Islands and juvenile fish from the northeastern Bering Sea. We did not include any adults in our current study, and a geographic range did not exist. Therefore, this comparison may not be ideal. However, this comparison highlights the possibility that these fractionation equations could be species- or region specific. It also highlights the value of controlled-temperature studies that are able to measure salinity and to factor out other sources of variability, such as ontogeny and geographic factors.

The $\delta^{18}O_o$ fractionation equations in Table 2 are from a wide variety of species, but have slopes that only show slight variation; however, the intercepts display greater variability. We chose the variety of species for a number of reasons. First, all the species and studies listed are from controlled laboratory rearing environments using fish in early life stages, as was the case in our study. Second, the wide variety provided for comparisons that were likely to demonstrate differences. Third, the list of studies, and species, was limited because many historic studies did not make the correct conversion of $\delta^{18}O_w$ on the VSMOW scale to the VPDB scale. When comparing the congeneric species, Pacific cod and Atlantic cod, in the 1000 ln α fractionation equation form, the slopes were different by a small margin, but the intercepts were very different. Pacific cod has a much higher intercept than Atlantic cod, the highest of all gadids in Table 2, while Atlantic cod has the second lowest intercept among the gadids. The most striking differences are between the biologically divergent anadromous and catadromous species. Among the species in Table 2, in the 1000 ln α form, the often-called semi-anadromous species delta smelt *Hypomesus transpacificus* and the anadromous Arctic charr *Salvelinus alpinus* have by a large margin the lowest intercepts, and their slopes are the highest. In comparison, the catadromous species glass eel *Anguilla japonica* has by a large margin the highest intercept and by a small margin the lowest slope. If the glass eel's regression parameters were estimated with similar SEs to that of delta smelt or Arctic charr (Table 2), these differences cannot be explained by the estimated parameter errors alone. The estimated slopes and intercepts of these anadromous or semi-anadromous and catadromous species span a greater range than the estimated parameters of the marine species. As such, the results of the ANCOVA, which indicated no significant differences among the 4 gadid fractionation equations in the current study, should not be surprising given that they are all gadids. Other researchers, such as Sakamoto et al. (2017), also noted a broad similarity of fractionation equation slopes and often different intercepts. In Eqs. (1) & (3), the $\delta^{18}O_w$ is a scaler on the *y*-axis; hence, any problems in estimating or measuring $\delta^{18}O_w$ would cause variations in the intercepts (Hoie et al. 2004, Dorval et al. 2011, Hanson et al. 2013). Alternatively, the differences could indicate species-specific non-equilibrium water to aragonite $\delta^{18}O_o$ fractionation. In a thorough summary of this alternative, Darnaude et al. (2014) suggested that if vital effects (physiological and metabolic influences) vary between species, then species-specific fractionation equations are necessary. This point is highlighted by the stenothermic versus eurythermic differences between Arctic cod and saffron cod and is also confirmed in published studies where large differences in fractionation equations were seen between anadromous and catadromous species (Godiksen et al. 2010, Shirai et al. 2018, Willmes et al. 2019) and the controlled laboratory studies listed in Table 2. After comparisons of our 4 gadid species-specific fractionation equations with published equations, we conclude that species-specific fractionation equations are necessary for accurate application of this technique to questions of thermographic, paleotemperature reconstructions or fisheries ecology.

5. CONCLUSIONS

Changing ocean temperatures are dramatically affecting marine ecosystems, so understanding temperature or habitat preference is important for managing marine resources. Developing species-specific $\delta^{18}O_o$ fractionation equations is critical to understanding the thermal history of fish and how their growth or metabolic function is reacting to the changing marine ecosystems. In developing these $\delta^{18}O_o$ fractionation equations, a particular strength of this study was that the 4 gadid species from the North Pacific and Arctic oceans were evaluated under common experimental conditions. Otoliths along with accurate $\delta^{18}O_o$ fractionation equations also provide us tools to reconstruct fish temperature histories and understand the effects of temperature on fish recruitment. For example, the relationship between temperature histories can be paired with fish energetic analyses and trophic biomarker content to provide a mechanistic link between changing thermal fields, fish condition, and resultant recruitment strength. Reconstruction of tem-

perature histories can also help us understand fish growth, habitat use, and migration patterns. Ancient otoliths can be paired with accurate $\delta^{18}O_o$ fractionation equations to make paleotemperature estimates and to understand a species' thermal ecology over evolutionary time scales. However, a limitation of $\delta^{18}O_o$ temperature predictions, including paleotemperature reconstructions, is the need for $\delta^{18}O_w$ values or a proxy such as salinity in combination with a geolocation-specific salinity mixing line. The new $\delta^{18}O_o$ fractionation equations we estimated represent a unique situation where 4 gadid species, representing boreal and Arctic regions, were compared. We found that the fractionation equations themselves, from the gadid species, were not statistically different but were within a larger spectrum of diverse fractionation equations. The lack of a statistical difference between the 4 fractionation equations here does not negate the fact that there are ecological or biological differences between these gadid species. The test we performed with the wild-caught Arctic cod further indicated the importance of species-specific fractionation equations. Hence, the 4 new equations can be used to improve the estimates of temperature experienced by a fish or to gain a better understanding of how temperature affects the growth and ecology of fish. To our knowledge, this is the first study to enable such a direct comparison between 4 closely related species.

Acknowledgements. The authors thank staff in the Age and Growth Program at the Alaska Fisheries Science Center (AFSC) for support while doing this project. We thank Andy Ross at the Stable Isotope Laboratory of the College of Earth, Ocean, and Atmospheric Sciences, Oregon State University, for assistance in analyzing our samples. For the CTD data, we thank Jeanette Gann at AFSC, Seth Danielson at the University of Alaska, and Libby Logerwell at AFSC. We thank 2 University of Washington interns, Alyssa Scott and Sammy Anderson, for their assistance. For reviewing and commenting on this manuscript, the authors further thank Martin Dorn and Matt Wilson of AFSC. We are grateful to Mary Elizabeth (Beth) Matta at AFSC for producing the map in Fig. 1. We also thank Malte Willmes at the University of California, Davis, for a helpful review and 2 anonymous reviewers for their constructive comments. This project was supported with funding from the North Pacific Research Board Grant No. 1228 and 2014 Essential Fish Habitat funding from NOAA, AFSC. The findings and conclusions in the paper are those of the authors and do not necessarily represent the views of the National Marine Fisheries Service, NOAA. Reference to trade names does not imply endorsement by the National Marine Fisheries Service, NOAA

LITERATURE CITED

Andrews AH, Pacicco A, Allman R, Falterman BJ, Lang ET, Golet W (2020) Age validation of yellowfin (*Thunnus albacares*) and bigeye (*Thunnus obesus*) tuna of the northwestern Atlantic Ocean. Can J Fish Aquat Sci 77: 637–643

Barbeaux SJ, Holsman K, Zador S (2020) Marine heatwave stress test of ecosystem-based fisheries management in the Gulf of Alaska Pacific cod fishery. Front Mar Sci 7:1–21

Benson IM, Kastelle CR, Helser TE, Short JA, Anderl DM (2019) Age interpretation in eulachon (*Thaleichthys pacificus*) as suggested by otolith microchemical signatures. Environ Biol Fishes 102:629–643

Brand WA, Coplen TB, Rosner M, Prohaska T (2014) Assessment of international reference materials for isotope-ratio analysis (IUPAC Technical report). Pure Appl Chem 86:425–467

Brodeur RD, Busby MS, Wilson MT (1995) Summer distribution of early life stages of walleye pollock, *Theragra chalcogramma*, and associated species in the western Gulf of Alaska. Fish Bull (Wash D C) 93:603–618

Burrows MT, Schoeman DS, Richardson AJ, Molinos JG and others (2014) Geographical limits to species-range shifts are suggested by climate velocity. Nature 507:492–495

Campana SE (1999) Chemistry and composition of fish otoliths: pathways, mechanisms and applications. Mar Ecol Prog Ser 188:263–297

Campana SE, Thorrold SR (2001) Otoliths, increments, and elements: keys to a comprehensive understanding of fish populations? Can J Fish Aquat Sci 58:30–38

Conroy JL, Thompson DM, Cobb KM, Noone D, Rea S, Legrande AN (2017) Spatiotemporal variability in the $\delta^{18}O$–salinity relationship of seawater across the tropical Pacific Ocean. Paleoceanography 32:484–497

Copeman LA, Laurel BJ, Spencer M, Sremba A (2017) Temperature impacts on lipid allocation among juvenile gadid species at the Pacific Arctic–Boreal interface: an experimental laboratory approach. Mar Ecol Prog Ser 566:183–198

Copeman L, Spencer M, Heintz R, Vollenweider J and others (2020) Ontogenetic patterns in lipid and fatty acid biomarkers of juvenile polar cod (*Boreogadus saida*) and saffron cod (*Eleginus gracilis*) from across the Alaska Arctic. Polar Biol 43:1121–1140

Darnaude AM, Hunter E (2018) Validation of otolith $\delta^{18}O$ values as effective natural tags for shelf-scale geolocation of migrating fish. Mar Ecol Prog Ser 598:167–185

Darnaude AM, Sturrock A, Trueman CN, EIMF, Mouillot D, Campana SE, Hunter E (2014) Listening in on the past: What can otolith $\delta^{18}O$ values really tell us about the environmental history of fishes? PLOS ONE 9:e108539

Degens ET, Deuser WG, Haedrich RL (1969) Molecular structure and composition of fish otoliths. Mar Biol 2:105–113

Dorval E, Piner K, Robertson L, Reiss CS, Javor B, Vetter R (2011) Temperature record in the oxygen stable isotopes of Pacific sardine otoliths: experimental vs. wild stocks from the Southern California Bight. J Exp Mar Biol Ecol 397:136–143

Drost HE, Lo M, Carmack EC, Farrell AP (2016) Acclimation potential of Arctic cod (*Boreogadus saida*) from the rapidly warming Arctic Ocean. J Exp Biol 219:3114–3125

Elsdon TS, Wells BK, Campana SE, Gillanders BM and others (2008) Otolith chemistry to describe movements and life-history parameters of fishes: hypotheses, assumptions, limitations and inferences. In: Gibson RN, Atkinson RJA, Gordon JDM (eds) Oceanography and marine biology: an annual review, Vol 46, Book 46. CRC Press, Boca Raton, FL, p 297–330

Fairbanks RG (1982) The origin of continental shelf and slope water in the New York Bight and Gulf of Maine: evidence from $H_2{}^{18}O/H_2{}^{16}O$ ratio measurements. J Geophys Res 87:5796–5808

Fissel B, Dalton M, Garber-Yonts B, Haynie A and others (2019) Stock assessment and fishery evaluation report for the groundfish fisheries of the Gulf of Alaska and Bering Sea/Aleutian Islands area: economic status of the groundfish fisheries off Alaska, 2018. North Pacific Fishery Management Council, Anchorage, AK

Fossheim M, Primicerio R, Johannesen E, Ingvaldsen RB, Aschan MM, Dolgov AV (2015) Recent warming leads to a rapid borealization of fish communities in the Arctic. Nat Clim Chang 5:673–677

Friedman I, O'Neil JR (1977) Compilation of stable isotope fractionation factors of geochemical interests. In: Fleischer M (ed) Data of geochemistry, 6th edn. Geological Survey Professional Paper 440-KK. US Geological Survey, Washington, DC

Gao YW, Schwarcz HP, Brand U, Moksness E (2001) Seasonal stable isotope records of otoliths from ocean-pen reared and wild cod, *Gadus morhua*. Environ Biol Fishes 61:445–453

Geffen AJ (2012) Otolith oxygen and carbon stable isotopes in wild and laboratory-reared plaice (*Pleuronectes platessa*). Environ Biol Fishes 95:419–430

Geffen AJ, Hoie H, Folkvord A, Hufthammer AK and others (2011) High-latitude climate variability and its effect on fisheries resources as revealed by fossil cod otoliths. ICES J Mar Sci 68:1081–1089

Gerdeaux D, Dufour E (2012) Inferring occurrence of growth checks in pike (*Esox lucius*) scales by using sequential isotopic analysis of otoliths. Rapid Commun Mass Spectrom 26:785–792

Godiksen J, Svenning MA, Dempson JB, Marttila M, Storm-Suke A, Power M (2010) Development of a species-specific fractionation equation for Arctic charr (*Salvelinus alpinus* (L.)): an experimental approach. Hydrobiologia 650:67–77

Hane Y, Kimura S, Yokoyama Y, Miyairi Y and others (2020) Reconstruction of temperature experienced by Pacific bluefin tuna *Thunnus orientalis* larvae using SIMS and microvolume CF-IRMS otolith oxygen isotope analyses. Mar Ecol Prog Ser 649:175–188

Hanson NN, Wurster CM, EIMF, Todd CD (2013) Reconstructing marine life-history strategies of wild Atlantic salmon from the stable isotope composition of otoliths. Mar Ecol Prog Ser 475:249–266

Harwood AJP, Dennis PF, Marca AD, Pilling GM, Millner RS (2008) The oxygen isotope composition of water masses within the North Sea. Estuar Coast Mar Sci 78:353–359

Helser TE, Colman JR, Anderl DM, Kastelle CR (2017) Growth dynamics of saffron cod (*Eleginus gracilis*) and Arctic cod (*Boreogadus saida*) in the northern Bering and Chukchi seas. Deep Sea Res II 135:66–77

Helser T, Kastelle C, Crowell A, Ushikubo T, Orland IJ, Kozdon R, Valley JW (2018a) A 200-year archaeozoological record of Pacific cod (*Gadus macrocephalus*) life history as revealed through ion microprobe oxygen isotope ratios in otoliths. J Archaeol Sci 21:1236–1246

Helser TE, Kastelle CR, McKay JL, Orland IJ, Kozdon R, Valley JW (2018b) Evaluation of micromilling/conventional isotope ratio mass spectrometry and secondary ion mass spectrometry of $\delta^{18}O$ values in fish otoliths for sclerochronology. Rapid Commun Mass Spectrom 32:1781–1790

Higuchi T, Ito S, Ishimura T, Kamimura Y and others (2019) Otolith oxygen isotope analysis and temperature history in early life stages of the chub mackerel *Scomber japonicus* in the Kuroshio–Oyashio transition region. Deep Sea Res II 169–170:104660

Hoegh-Guldberg O, Bruno JF (2010) The impact of climate change on the world's marine ecosystems. Science 328: 1523–1528

Hoie H, Folkvord A (2006) Estimating the timing of growth rings in Atlantic cod otoliths using stable oxygen isotopes. J Fish Biol 68:826–837

Hoie H, Folkvord A, Otterlei E (2003) Effect of somatic and otolith growth rate on stable isotopic composition of early juvenile cod (*Gadus morhua* L) otoliths. J Exp Mar Biol Ecol 289:41–58

Hoie H, Otterlei E, Folkvord A (2004) Temperature-dependent fractionation of stable oxygen isotopes in otoliths of juvenile cod (*Gadus morhua* L.). ICES J Mar Sci 61:243–251

Hollowed AB, Planque B, Loeng H (2013) Potential movement of fish and shellfish stocks from the sub-Arctic to the Arctic Ocean. Fish Oceanogr 22:355–370

Horn PL, Neil HL, Paul LJ, McMillan PJ (2012) Age verification, growth and life history of rubyfish *Plagiogeneion rubiginosum*. Mar Freshw Res 46:353–368

Hussy K, Mosegaard H, Jessen F (2004) Effect of age and temperature on amino acid composition and the content of different protein types of juvenile Atlantic cod (*Gadus morhua*) otoliths. Can J Fish Aquat Sci 61:1012–1020

Jones JB, Campana SE (2009) Stable oxygen isotope reconstruction of ambient temperature during the collapse of a cod (*Gadus morhua*) fishery. Ecol Appl 19:1500–1514

Kalish JM (1991) Oxygen and carbon stable isotopes in the otoliths of wild and laboratory-reared Australian salmon (*Arripis trutta*). Mar Biol 110:37–47

Kastelle CR, Helser TE, McKay JL, Johnston CG, Anderl DM, Matta ME, Nichol DG (2017) Age validation of Pacific cod (*Gadus macrocephalus*) using high-resolution stable oxygen isotope ($\delta^{18}O$) chronologies in otoliths. Fish Res 185:43–53

Kastelle C, Helser T, TenBrink T, Hutchinson C, Goetz B, Gburski C, Benson I (2020) Age validation of four rockfishes (genera *Sebastes* and *Sebastolobus*) with bomb-produced radiocarbon. Mar Freshw Res 71:1355–1366

Kim ST, Mucci A, Taylor BE (2007) Phosphoric acid fractionation factors for calcite and aragonite between 25 and 75 °C: revisited. Chem Geol 246:135–146

Koenker BL, Copeman LA, Laurel BJ (2018) Impacts of temperature and food availability on the condition of larval Arctic cod (*Boreogadus saida*) and walleye pollock (*Gadus chalcogrammus*). ICES J Mar Sci 75:2370–2385

Laurel BJ, Ryer CH, Knoth B, Stoner AW (2009) Temporal and ontogenetic shifts in habitat use of juvenile Pacific cod (*Gadus macrocephalus*). J Exp Mar Biol Ecol 377: 28–35

Laurel BJ, Knoth BA, Ryer CH (2016a) Growth, mortality, and recruitment signals in age-0 gadids settling in coastal Gulf of Alaska. ICES J Mar Sci 73:2227–2237

Laurel BJ, Spencer M, Iseri P, Copeman LA (2016b) Temperature-dependent growth and behavior of juvenile Arctic cod (*Boreogadus saida*) and co-occurring North Pacific gadids. Polar Biol 39:1127–1135

Laurel BJ, Copeman LA, Spencer M, Iseri P (2018) Comparative effects of temperature on rates of development and survival of eggs and yolk-sac larvae of Arctic cod (*Bore-*

ogadus saida) and walleye pollock (*Gadus chalcogrammus*). ICES J Mar Sci 75:2403–2412

Logerwell E, Busby M, Carothers C, Cotton S and others (2015) Fish communities across a spectrum of habitats in the western Beaufort Sea and Chukchi Sea. Prog Oceanogr 136:115–132

Logerwell E, Rand K, Danielson S, Sousa L (2018) Environmental drivers of benthic fish distribution in and around Barrow Canyon in the northeastern Chukchi Sea and western Beaufort Sea. Deep Sea Res II 152:170–181

Matta ME, Miller JA, Short JA, Heiser TE, Hurst TP, Rand KM, Ormseth OA (2019) Spatial and temporal variation in otolith elemental signatures of age-0 Pacific cod (*Gadus macrocephalus*) in the Gulf of Alaska. Deep Sea Res II 165:268–279

Miller JA, Banks MA, Gomez-Uchida D, Shanks AL (2005) A comparison of population structure in black rockfish (*Sebastes melanops*) as determined with otolith microchemistry and microsatellite DNA. Can J Fish Aquat Sci 62:2189–2198

Mueter FJ, Weems J, Farley EV, Sigler MF (2017) Arctic ecosystem integrated survey (Arctic Eis): marine ecosystem dynamics in the rapidly changing Pacific Arctic Gateway. Deep Sea Res II 135:1–6

Popper AN, Ramcharitar J, Campana SE (2005) Why otoliths? Insights from inner ear physiology and fisheries biology. Mar Freshw Res 56:497–504

Sakamoto T, Komatsu K, Yoneda M, Ishimura T and others (2017) Temperature dependence of $\delta^{18}O$ in otolith of juvenile Japanese sardine: laboratory rearing experiment with micro-scale analysis. Fish Res 194:55–59

Schwarcz HP, Gao Y, Campana S, Browne D, Knyf M, Brand U (1998) Stable carbon isotope variations in otoliths of Atlantic cod (*Gadus morhua*). Can J Fish Aquat Sci 55: 1798–1806

Sharp Z (2007) Principles of stable isotope geochemistry. Prentice Hall, Hoboken, NJ

Shimada AM, Kimura DK (1994) Seasonal movements of Pacific cod, *Gadus macrocephalus*, in the eastern Bering Sea and adjacent waters based on tag-recapture data. Fish Bull (Wash D C) 92:800–816

Shirai K, Otake T, Amano Y, Kuroki M and others (2018) Temperature and depth distribution of Japanese eel eggs estimated using otolith oxygen stable isotopes. Geochim Cosmochim Acta 236:373–383

Spero HJ, Lea DW (1996) Experimental determination of stable isotope variability in *Globigerina bulloides*: implications for paleoceanographic reconstructions. Mar Micropaleontol 28:231–246

Storm-Suke A, Dempson JB, Reist JD, Power M (2007) A field-derived oxygen isotope fractionation equation for *Salvelinus* species. Rapid Commun Mass Spectrom 21: 4109–4116

Thomas ORB, Swearer SE (2019) Otolith biochemistry — a review. Rev Fish Sci Aquacult 27:458–489

Thomas ORB, Swearer SE, Kapp EA, Peng P and others (2019) The inner ear proteome of fish. FEBS J 286:66–81

Thorrold SR, Campana SE, Jones CM, Swart PK (1997) Factors determining $\delta^{13}C$ and $\delta^{18}O$ fractionation in aragonitic otoliths of marine fish. Geochim Cosmochim Acta 61:2909–2919

Tracey DM, Andrews AH, Horn PL, Neil HL (2017) Another New Zealand centenarian: age validation of black cardinalfish (*Epigonus telescopus*) using lead–radium and bomb radiocarbon dating. Mar Freshw Res 68:352–360

Vestfals CD, Ciannelli L, Hoff GR (2016) Changes in habitat utilization of slope-spawning flatfish across a bathymetric gradient. ICES J Mar Sci 73:1875–1889

Vestfals CD, Mueter FJ, Duffy-Anderson JT, Busby MS, De Robertis A (2019) Spatio-temporal distribution of polar cod (*Boreogadus saida*) and saffron cod (*Eleginus gracilis*) early life stages in the Pacific Arctic. Polar Biol 42: 969–990

von Leesen G, Ninnemann US, Campana SE (2020) Stable oxygen isotope reconstruction of temperature exposure of the Icelandic cod (*Gadus morhua*) stock over the last 100 years. ICES J Mar Sci 77:942–952

Weidel BC, Ushikubo T, Carpenter SR, Kita NT and others (2007) Diary of a bluegill (*Lepomis macrochirus*): daily $\delta^{13}C$ and $\delta^{18}O$ records in otoliths by ion microprobe. Can J Fish Aquat Sci 64:1641–1645

Weidman CR, Millner R (2000) High-resolution stable isotope records from North Atlantic cod. Fish Res 46:327–342

West CF, Wischniowski S, Johnston C (2012) Pacific cod (*Gadus macrocephalus*) as a paleothermometer: otolith oxygen isotope reconstruction. J Archaeol Sci 39: 3277–3283

Willmes M, Lewis LS, Davis BE, Loiselle L and others (2019) Calibrating temperature reconstructions from fish otolith oxygen isotope analysis for California's critically endangered delta smelt. Rapid Commun Mass Spectrom 33: 1207–1220

Wright JD (2013) Global climate change in marine stable isotope records. In: Noller JS, Sowers JM, Lettis WR (eds) Quaternary geochronology: methods and applications. American Geophysical Union, Washington, DC, p 671–682

Wright PJ, Panfili J, Morales-Nin B, Geffen AJ (2002) Otoliths. In: Panfili J, de Pontual H, Troadec H, Wright PJ (eds) Manual of fish sclerochronology. IFREMER-IRD, Brest, p 31–57

Yamamoto-Kawai M, Carmack EC, McLaughlin FA, Falkner KK (2010) Oxygen isotope ratio, barium and salinity in waters around the North American coast from the Pacific to the Atlantic: implications for freshwater sources to the Arctic throughflow. J Mar Res 68:97–117

Editorial responsibility: Jana Davis, Annapolis, Maryland, USA
Reviewed by: M. Willmes and 2 anonymous referees

Submitted: February 6, 2021
Accepted: December 23, 2021
Proofs received from author(s): March 7, 2022